NASA-CR-194296

NAG 1-776

185441

IN-02-CR

17P

# CALCULATION OF HYPERSONIC SHOCK STRUCTURE USING FLUX-SPLIT ALGORITHMS

W.M. Eppard
B. Grossman

ICAM REPORT 91-07-04

Interdisciplinary Center for Applied Mathematics
Virginia Polytechnic Institute and State University
Blacksburg, VA 24061

July 1991

(NASA-CR-194296) CALCULATION OF HYPERSONIC SHOCK STRUCTURE USING FLUX-SPLIT ALGORITHMS (Virginia Polytechnic Inst. and State Univ.) 17 p

N94-13607

Unclas

G3/02 0185441

# Calculation of Hypersonic Shock Structure Using Flux-Split Algorithms

W. M. Eppard and B. Grossman

Department of Aerospace and Ocean Engineering,
Virginia Polytechnic Institute and State University,
Blacksburg, Virginia 24061

## Introduction

There exists an altitude regime in the atmosphere that is within the continuum domain, but wherein the conventional Navier-Stokes equations cease to be accurate. The altitude limits for this so called continuum transition regime depend on vehicle size and speed.[1] Within this regime the thickness of the bow shock wave is no longer negligible when compared to the shock stand-off distance and the peak radiation intensity occurs within the shock wave structure itself. For this reason it is no longer valid to treat the shock wave as a discontinuous jump and it becomes necessary to compute through the shock wave itself. To accurately calculate hypersonic flowfields, the governing equations must be capable of yielding realistic profiles of flow variables throughout the structure of a hypersonic shock wave.[2]

The conventional form of the Navier-Stokes equations is restricted to flows with only small departures from translational equilibrium; it is for this reason they do not provide the capability to accurately predict hypersonic shock structure. Calculations in the continuum transition regime, therefore, require the use of governing equations other than Navier-Stokes. In this paper several alternatives to Navier-Stokes are discussed; first for the case of a monatomic gas and then for the case of a diatomic gas where rotational energy must be included. Results are presented for normal shock calculations with argon and nitrogen.

## Navier-Stokes Equations

The study of flow with translational non-equilibrium is largely concerned with attempts to solve the Boltzmann equation

$$\frac{\partial}{\partial t}(nf) + c_i \frac{\partial}{\partial x_i}(nf) + \frac{\partial}{\partial c_i}(X_i nf) = \left\{ \frac{\partial}{\partial t}(nf) \right\}_{coll}, \tag{1}$$

where $c_i$ is the particle velocity, $f$ is the velocity distribution function $f(c_i, x_i, t)$, and $X_i$ is the external force per unit mass acting on a particle.[3] Unfortunately, this equation is difficult to solve for the general case and approximate methods are required.

One such method, the Chapman-Enskog expansion, is an expansion of the distribution function about translational equilibrium in terms of the Knudsen number ($\xi = \lambda/L$) as follows

$$f = f_o(1 + \xi\phi_1 + \xi^2\phi_2 + \dots\ ). \tag{2}$$

The zeroth-order solution ($\xi \to 0$) corresponds to translational equilibrium and the governing equations reduce to the Euler equations. In retaining first-order terms in $\xi$ we obtain

the Navier-Stokes equations. The Navier-Stokes equations in one spatial dimension are given as

$$\frac{\partial \mathbf{Q}}{\partial t} + \frac{\partial}{\partial x}(\mathbf{F} + \mathbf{F}_v) = \mathbf{0}\,, \tag{3}$$

where

$$\mathbf{Q} = \begin{pmatrix} \rho \\ \rho u \\ \rho e_0 \end{pmatrix}, \qquad \mathbf{F} = \begin{pmatrix} \rho u \\ \rho u^2 + p \\ \rho u h_0 \end{pmatrix}, \qquad \mathbf{F}_v = \begin{pmatrix} 0 \\ -\tau \\ q - \tau u \end{pmatrix}. \tag{4a, b, c}$$

Here, $\rho$ is the mass density, $p$ is the pressure, and $u$ is the velocity in the $x$ direction. The internal energy per unit mass is denoted as $e$, with the total energy per unit mass $e_0 = e + u^2/2$ and total enthalpy per unit mass $h_0 = e_0 + p/\rho$. The shear stress and heat flux terms for this one spatial dimension are given as

$$\tau = \tau_1 = \frac{4}{3}\mu\frac{\partial u}{\partial x}\,, \tag{5}$$

$$q = q_1 = -k\frac{\partial T}{\partial x}\,, \tag{6}$$

where $T$ is the translational temperature.

It is important to note that the derivation of the Navier-Stokes equations from Chapman-Enskog theory proves, rather than assumes, that Stokes hypothesis ($\mu_B = 0$) holds for a monatomic gas.[3] Furthermore, Chapman-Enskog theory allows for a theoretical means of determining viscosity. For an inverse power molecule with an intermolecular repulsive force given by

$$F = \frac{\kappa}{r^\eta}\,, \tag{7}$$

a relationship exists between the coefficient of viscosity $\mu$ and the translational temperature and is given as [4]

$$\mu = \mu_0\left(\frac{T}{T_0}\right)^{\left(\frac{1}{2}+\frac{2}{\eta-1}\right)} = \mu_0\left(\frac{T}{T_0}\right)^{\omega}. \tag{8}$$

Within the same set of assumptions, the coefficient of thermal conductivity may be written as

$$k = \frac{5}{2}\mu c_{v\,tr}\,. \tag{9}$$

## Burnett Equations

Retention of the second-order terms in $\xi$ yields what are known as the Burnett equations. These equations should produce more accurate solutions for flows with large deviations from translational equilibrium and will allow meaningful calculations in the continuum transition regime. The Burnett equations for one spatial dimension are of the same form as the Navier-Stokes equations except that the closure relations are given as

$$\tau = \tau_1 + \tau_2 \tag{10}$$

and

$$q = q_1 + q_2 \,, \tag{11}$$

where

$$\begin{aligned}\tau_2 = &-\frac{\mu^2}{p}\Big[(\frac{2}{3}\omega_1 - \frac{14}{9}\omega_2 + \frac{2}{9}\omega_6)(\frac{\partial u}{\partial x})^2 - \frac{2}{3}\omega_2\frac{RT}{\rho}\frac{\partial^2 u}{\partial x^2} + \frac{2}{3}\omega_2\frac{RT}{\rho^2}(\frac{\partial \rho}{\partial x})^2 \\ &- \frac{2}{3}(\omega_2 - \omega_4)\frac{R}{\rho}\frac{\partial \rho}{\partial x}\frac{\partial T}{\partial x} + \frac{2}{3}(\omega_4 + \omega_5)\frac{R}{T}(\frac{\partial T}{\partial x})^2 - \frac{2}{3}(\omega_2 - \omega_3)R\frac{\partial^2 T}{\partial x^2}\Big] \,,\end{aligned} \tag{12}$$

$$q_2 = \frac{\mu^2}{\rho}\Big[(\theta_1 + \frac{8}{3}\theta_2 + \frac{2}{3}\theta_3 + \frac{2}{3}\theta_5)\frac{1}{T}\frac{\partial u}{\partial x}\frac{\partial T}{\partial x} + \frac{2}{3}(\theta_2 + \theta_4)\frac{\partial^2 u}{\partial x^2} + \frac{2}{3}\theta_3\frac{1}{\rho}\frac{\partial u}{\partial x}\frac{\partial \rho}{\partial x}\Big] \,, \tag{13}$$

and the $\omega_i$'s and $\theta_i$'s are constants determined from Chapman-Enskog theory and depend on the constant $\eta$ in the inverse power model. [4]

One drawback of the Burnett equations, other than their complexity, is that they tend to become unstable as mesh spacing is refined. This problem has been overcome by adding selected terms from the third-order Super-Burnett equations that have a stabilizing effect. [5] Hence, the Burnett equations are solved as

$$\tau = \tau_1 + \tau_2 + \tau_3^{'} \tag{14}$$

and

$$q = q_1 + q_2 + q_3^{'} \,, \tag{15}$$

where

$$\tau_3^{'} = -\frac{\mu^3}{p^2}(\frac{2}{9}RT\frac{\partial^3 u}{\partial x^3}) \tag{16}$$

and

$$q_3^{'} = \frac{\mu^3}{p\rho}(\frac{11}{16}R\frac{\partial^3 T}{\partial x^3} - \frac{5}{8}\frac{RT}{\rho}\frac{\partial^3 \rho}{\partial x^3}) \,. \tag{17}$$

Here, $\tau_3^{'}$ and $q_3^{'}$ are the selected higher-order Super Burnett terms added for stability. [5]

## Rotational Energy

The Navier-Stokes and Burnett equations are valid for monatomic gases only. For diatomic gases some means must be included to account for molecular rotation. Inclusion of molecular rotation from first principles requires a distribution function involving not only the coordinates of the molecule and its linear velocity, but also its rotational energy. The corresponding Boltzmann equation must also be modified so that the right-hand side includes a mechanism for energy exchange between the translational and rotational energy modes during collisions. [4] Wang Chang and Uhlenbeck [6] were the first to carry out the Chapman-Enskog expansion to first order for such a system. For cases where the relaxation time for rotation is sufficiently small such that rotational and translational energies are at all times near their equilibrium values, the system yields the Navier-Stokes equations plus

an additional bulk viscosity term ($\mu_B \nabla \cdot V$). This case is termed *easy exchange* and for one spatial dimension results in

$$\tau = \tau_1 + \tau_{1B}\,, \tag{18}$$

where

$$\tau_{1B} = \mu_B \frac{\partial u}{\partial x} \tag{19}$$

and $q = q_1$, where

$$k = \frac{5}{2}\mu c_{vtr} + \mu c_{vr}\,. \tag{20}$$

For cases where the relaxation time for rotation is significant and large deviations from rotational equilibrium occur (termed *difficult exchange*) the system results in the Navier-Stokes equations with $\rho e_0 = \rho(e_{tr} + e_r + u^2/2)$ plus an additional equation describing the relaxation of rotational energy

$$\frac{\partial e_r}{\partial t} = \frac{\hat{e}_r - e_r}{Z_r \tau_c}\,. \tag{21}$$

Here, $\hat{e}_r$ is the rotational energy at thermal equilibrium. The vibrational energy contribution to the internal energy has been neglected for two reasons. Firstly, only cases where the initial conditions are such that vibrational energy is negligible are considered, and secondly, for most shocks, the vibrational energy mode requires many collisions to reach equilibrium (on the order of $10^5$) and is essentially frozen throughout the shock. Electronic energy contribution to the internal energy has also been neglected. The value $Z_r$ is known as the rotational collision number and the functional form is given as [11]

$$Z_r = Z_r^{\infty} \Big/ \left[1. + \frac{\pi^{3/2}}{2}\left(\frac{T^*}{T}\right)^{1/2} + \left(\frac{\pi^2}{4} + \pi\right)\left(\frac{T^*}{T}\right)\right] \tag{22}$$

and $\tau_c$ is the mean collision time given as

$$\tau_c = \frac{\pi \mu}{4p}\,. \tag{23}$$

For one spatial dimension the governing equations for difficult exchange are given as

$$\frac{\partial \mathbf{Q}}{\partial t} + \frac{\partial}{\partial x}(\mathbf{F} + \mathbf{F}_v) = \mathbf{W}_s\,, \tag{24}$$

where

$$\mathbf{Q} = \begin{pmatrix} \rho \\ \rho u \\ \rho e_r \\ \rho e_0 \end{pmatrix}, \quad \mathbf{F} = \begin{pmatrix} \rho u \\ \rho u^2 + p \\ \rho e_r u \\ \rho u h_0 \end{pmatrix}, \quad \mathbf{F}_v = \begin{pmatrix} 0 \\ -\tau \\ q_r \\ q + q_r - \tau u \end{pmatrix}, \quad \mathbf{W}_s = \begin{pmatrix} 0 \\ 0 \\ \rho \dot{e}_r \\ 0 \end{pmatrix}. \tag{25a, b, c, d}$$

Here, $\tau = \tau_1$, $q = q_1$, where

$$k = \frac{5}{2}\mu c_{vtr} \tag{26}$$

and

$$q_r = -k_r \frac{\partial T_r}{\partial x}, \tag{27}$$

where

$$k_r = \mu c_{vr}. \tag{28}$$

At present no one has carried out the Chapman-Enskog expansion to second order for a gas possessing rotational energy.[4] However, one obtains reasonably good results if the Burnett equations are used in conjunction with either of the two cases above for easy or difficult energy exchange.

### Bulk Viscosity Model

As previously mentioned, when the energy exchange between rotation and translation occurs freely ($\tau_r$ is sufficiently small) the presence of rotational energy leads to the addition of a bulk viscosity term. This term appears in the stress components of the Navier-Stokes equations as follows

$$\sigma_{ij} = -\hat{p}\delta_{ij} + \mu(\frac{\partial u_i}{\partial x_j} + \frac{\partial u_j}{\partial x_i} - \frac{2}{3}\frac{\partial u_k}{\partial x_k}\delta_{ij}) + \mu_B \frac{\partial u_k}{\partial x_k}\delta_{ij}, \tag{29}$$

where $\hat{p}$ is the pressure corresponding to thermal equilibrium at $T$. It is important to note that bulk viscosity becomes important only when compressibility effects are present since $\mu_B$ appears only with the divergence of the velocity vector.[3] From kinetic theory we have

$$\sigma_{ij} = - < c_i' c_j' >, \tag{30}$$

$$p = \frac{1}{3}\rho < c_i'^2 >, \tag{31}$$

and

$$e_{tr} = \frac{1}{2} < c_i'^2 > . \tag{32}$$

Here, the brackets <> represent a moment of the distribution function, $c_i'$ is the thermal velocity, and p is the kinetic pressure which is valid in thermal non-equilibrium. It follows that

$$-\frac{\sigma_{ii}}{3} = p = \hat{p} - \mu_B(\nabla \cdot V) \tag{33}$$

and likewise

$$\frac{2}{3}\rho e_{tr} = \frac{2}{3}\rho \hat{e}_{tr} - \mu_B(\nabla \cdot V), \tag{34}$$

where $\hat{e}_{tr}$ is the translational energy at thermal equilibrium. It now becomes apparent that the bulk viscosity is a relaxation phenomenon resulting from the lag in adjustment to equilibrium of the rotational mode.[7] For example, when a gas is expanded there will be a reduction in the internal energy ($e$). This reduction will initially come entirely from the translational modes (fast modes) and only after some relaxation time will the translational

and rotational modes reach equilibrium at $T$. During this time the kinetic pressure is lower than that for thermal equilibrium and this is consistent with the equation above since $(\nabla \cdot V) > 0$. A similar process occurs for a compression.

To develop an expression for the bulk viscosity, consider a small volume of gas ($\delta Vol$) undergoing an expansion or compression as in Ref. 7. Considering only the work done by pressure the change in internal energy in a short time $t^*$ is given as

$$-\frac{p}{\rho}(\nabla \cdot V)t^* . \tag{35}$$

It is noted that in thermal equilibrium, for cases where vibrational and electronic energy contributions to the internal energy are negligible, $e_{tr} = 3/5e$ and $e_r = 2/5e$. In an expansion where thermal equilibrium is maintained $e_{tr}$ decreases by the amount

$$-\frac{3}{5}\frac{p}{\rho}(\nabla \cdot V)t^* \tag{36}$$

and $e_r$ decreases by the amount

$$-\frac{2}{5}\frac{p}{\rho}(\nabla \cdot V)t^* . \tag{37}$$

In an expansion where there is a lag in the rotational mode the entire loss of energy will initially come from the translational mode such that

$$e_{tr} = \hat{e}_{tr} - \frac{2}{5}\frac{p}{\rho}(\nabla \cdot V)t^* . \tag{38}$$

In comparison with equation (34) in terms of bulk viscosity it follows that

$$\mu_B = \frac{4}{15}p\,t^* . \tag{39}$$

It can be shown [7] that $t^*$ is approximately the relaxation time for rotation and taken as

$$\tau_r = Z_r \tau_c , \tag{40}$$

which is the relaxation time in the rotational model of the previous section.

## Numerical Issues

An implicit Steger-Warming type flux-splitting algorithm as in Ref. 8 was used to march in time to the steady-state solution. In Ref. 8 a general splitting was developed for a one-dimensional, vibrationally-relaxing, chemically reacting flow where it was shown that

$$\mathbf{F} = \mathbf{A}\mathbf{Q} = \left[\mathbf{T}(\mathbf{\Lambda}^+ + \mathbf{\Lambda}^-)\mathbf{T}^{-1}\right]\mathbf{Q} = \mathbf{F}^+ + \mathbf{F}^- . \tag{41}$$

Here, $\mathbf{Q}$ is the vector of conserved variables, and $\mathbf{F}$ is the flux vector given as

$$\mathbf{Q} = \begin{pmatrix} \rho_1 \\ \rho_2 \\ \vdots \\ \rho_N \\ \rho u \\ \rho_1 e_{n1} \\ \vdots \\ \rho_M e_{nM} \\ \rho e_0 \end{pmatrix}, \qquad \mathbf{F} = \begin{pmatrix} \rho_1 u \\ \rho_2 u \\ \vdots \\ \rho_N u \\ \rho u^2 + p \\ \rho_1 e_{n1} u \\ \vdots \\ \rho_M e_{nM} u \\ \rho u h_0 \end{pmatrix}, \tag{42a, b}$$

$\mathbf{A}$ is the flux Jacobian $\partial\mathbf{F}/\partial\mathbf{Q}$, $\mathbf{\Lambda}$ is the diagonal matrix whose elements are the eigenvalues of $\mathbf{A}$, and it was shown that

$$\mathbf{F}^{\pm} = (\frac{\tilde{\gamma}-1}{\tilde{\gamma}})\rho\lambda_A{}^{\pm}\mathbf{F}_A + \frac{1}{2\tilde{\gamma}}\rho\lambda_B{}^{\pm}\mathbf{F}_B + \frac{1}{2\tilde{\gamma}}\rho\lambda_C{}^{\pm}\mathbf{F}_C\,, \tag{43}$$

where

$$\mathbf{F}_A = \begin{pmatrix} \rho_1/\rho \\ \rho_2/\rho \\ \vdots \\ \rho_N/\rho \\ u \\ \rho_1 e_{n1}/\rho \\ \vdots \\ \rho_M e_{nM}/\rho \\ h_0 - a^2/(\tilde{\gamma}-1) \end{pmatrix}, \qquad \mathbf{F}_{B,C} = \begin{pmatrix} \rho_1/\rho \\ \rho_2/\rho \\ \vdots \\ \rho_N/\rho \\ u \pm a \\ \rho_1 e_{n1}/\rho \\ \vdots \\ \rho_M e_{nM}/\rho \\ h_0 \pm ua \end{pmatrix}, \tag{44a, b}$$

and $\lambda_A = u$, $\lambda_B = u + a$, and $\lambda_C = u - a$. For the present application the rotational non-equilibrium model is used in place of the vibrational model of Ref. 8.

Both the Navier-Stokes and Burnett viscous fluxes are treated implicitly in a method similar to that of Ref. 9. Here, the coefficients in front of the derivative terms are frozen during the linearization. The source terms resulting from non-equilibrium rotation are also handled implicitly. An Euler implicit time integration method has been applied to the set of governing equations, resulting in the following semi-discrete form

$$\left[I\frac{\Delta x}{\Delta t} + \delta_x(\mathbf{A}^+ + \mathbf{A}^- + \frac{\partial\mathbf{F}_v}{\partial\mathbf{Q}})^n - \frac{\partial\mathbf{W}_s}{\partial\mathbf{Q}}\right]\Delta\mathbf{Q} = -\mathbf{R}(\mathbf{Q}^n)\,, \tag{45}$$

where

$$\Delta\mathbf{Q} = \mathbf{Q}^{n+1} - \mathbf{Q}^n\,, \tag{46}$$

$$\delta_x(\ ) = (\ )_{i+1/2} - (\ )_{i-1/2}\,, \tag{47}$$

and

$$\mathbf{R}(\mathbf{Q}^n) = \delta_x(\mathbf{F}^+ + \mathbf{F}^- + \mathbf{F}_v)^n - \mathbf{W}_s{}^n \Delta x. \tag{48}$$

A third-order, upwind biased extrapolation (in MUSCL form) is used for the inviscid fluxes in the right-hand side of equation (45), while a first order upwind extrapolation used for the inviscid Jacobians appearing in the left-hand side of equation (45). No limiting was necessary for any of the calculations presented. It is noted that Navier-Stokes calculations require a block tridiagonal inversion at each time step while Burnett calculations require a block pentadiagonal inversion at each time step.

Each solution was obtained on a grid consisting of 150 equally spaced mesh points. The initial condition was composed of three segments, a constant region initialized at the inflow conditions, an initial guess at the shock profile that blended between the inflow conditions and the conditions behind a normal shock, and finally a constant region at the conditions behind a normal shock. Characteristic boundary conditions were used at the outflow with the pressure at the exit set at that behind a normal shock.

In all the calculations presented the following expression is used as a reference length for shock structure

$$\lambda_1 = \frac{16\mu_1}{5\rho_1(2\pi R T_1)^{0.5}}. \tag{49}$$

This is the mean free path that would exist upstream of the shock if the gas were composed of hard elastic spheres. Also, for all calculations the coefficients in the Burnett equations are those corresponding to a hard sphere gas ($\eta = \infty, \omega = .5$) while $\omega = .72$ is used in the viscosity law for better agreement with experiment. In nitrogen calculations where the rotational non-equilibrium model is incorporated the constants $Z_r^\infty = 18.$ and $T^* = 91.5K$ are used. [4]

Density and temperature profiles are presented in a normalized fashion where

$$\rho_n = \frac{\rho - \rho_2}{\rho_2 - \rho_1}, \tag{50}$$

and

$$T_n = \frac{T - T_2}{T_2 - T_1}. \tag{51}$$

## Results

Results for argon shocks at Mach 20 and 35 are shown in Figures 1 and 2. Here, normalized temperature and density profiles are presented for Navier-Stokes and Burnett calculations as well as a Direct Simulation Monte Carlo solution (DSMC) as shown in Refs. 1 and 9. It is assumed that for these conditions the DSMC solution is essentially the valid solution. The density thicknesses predicted by the Burnett solution compare well with the DSMC results in both the Mach 20 an 35 cases. The Navier-Stokes density thicknesses are slightly less than the DSMC results. In the case of temperature thicknesses, the Burnett solution represents a significant improvement over the Navier-Stokes solution. Overall, it is seen for both cases that inclusion of the Burnett terms yields a significant improvement

over Navier-Stokes for both temperature an density profiles. Our results compare well with the shock calculations from Refs. 1 and 9.

Results for diatomic nitrogen at Mach 11 are shown in Figures 3 and 4. Figure 3 shows calculations with the Navier-Stokes equations alone, the Navier-Stokes equations with rotational non-equilibrium, and the Navier-Stokes equations with bulk viscosity, as well as the DSMC result from Ref. 4. Again, the DSMC solution is assumed to be valid. It is seen that the Navier-Stokes calculation alone produces density thicknesses that are too small. Navier-Stokes calculations with bulk viscosity and rotational non-equilibrium produce density profiles that compare very well with the DSMC calculation. In the case of temperature thicknesses, the Navier-Stokes calculation with bulk viscosity represents a slight improvement over Navier-Stokes calculations alone. The calculation with rotational non-equilibrium is able to capture the peak temperature in the shock, however, it is noted that in all cases the Navier-Stokes terms do not predict large enough temperature thicknesses. Ref. 4 did not present Navier-Stokes results for this case.

Figure 4 shows calculations with the Burnett equations alone, the Burnett equations with rotational non-equlibrium, and the Burnett equations with bulk viscosity, as well as the DSMC calculation from Ref. 4. It is seen that the Burnett calculation alone produces density thicknesses that are too small. Burnett calculations with bulk viscosity produce density profiles that compare very close to the DSMC calculation, and appear to be slightly better than the calculation with rotational non-equilibrium.

In the case of temperature thicknesses, the Burnett calculation with bulk viscosity represents a slight improvement over Burnett alone, and the calculation with rotational non-equilibrium very closely predicts the value and location of the peak temperature in the shock. The Burnett calculation with rotational non-equilibrium most closely matches the DSMC results. Our results for this case agree with the results from Ref. 4. Figures 5 and 6 show similar results in a Mach 6 shock for Nitrogen and these calculations agree well with the results from Ref. 10. In each case the Burnett calculations are more accurate than the Navier-Stokes calculations. The results obtained using the Navier-Stokes equations or Burnett equations in conjunction with a bulk viscosity model represents a new contribution. It is expected that the bulk viscosity results would be in better agreement with DSMC solutions for cases with smaller amounts of rotational non-equilibrium.

## Conclusions

In all cases the Burnett terms represent a considerable improvement over Navier-Stokes for both density and temperature profiles. For cases with rotational energy the Burnett equations with a bulk viscosity model represent an improvement over the Burnett equations alone, but do not contain a mechanism to predict the peak temperature within the shockwave. Navier-Stokes calculations with rotational non-equilibrium can predict the value and location of the peak temperature in the shock but suffer from inaccurate shock thickness. Burnett Calculations with rotational non-equilibrium produce the most accurate results of the continuum models tested.

**Acknowledgment**

This work was made possible by a grant from the NASA Langley Research Center, NAG-1-776, whose support is gratefully acknowledged.

**References**

1. K. A. Fiscko and D. R. Chapman, "Comparison of Burnett, Super-Burnett and Monte Carlo Solutions for Hypersonic Shock Structure," *16th International Symposium of Rarefied Gas Dynamics*, 1988.
2. D. R. Chapman, K. A. Fiscko, and F. E. Lumpkin, "Fundamental Problem in Computing Radiating Flow Fields with Thick Shock Waves," *Proceedings of SPIE*, Vol. 879, 106-112, 1988.
3. W. G. Vincenti and C. H. Kruger, Jr., "Introduction to Physical Gas Dynamics," Krieger, 1965.
4. F. E. Lumpkin III "Accuracy of the Burnett Equations for Hypersonic Real Gas Flows," AIAA Paper No. 91-0771, January, 1991.
5. X. Zong, R. W. MacCormack, and D. R. Chapman "Stabilization of the Burnett Equations and Application to High-Altitude Hypersonic Flows," AIAA Paper No. 91-0070, January, 1991.
6. Wang Chang, C. S. and G. E. Uhlenbeck, "Transport Phenomena in Polyatomic Gases," *CM-681, Engineering Research Institute, University of Michigan*, 1951.
7. S. Goldstein, "The Navier-Stokes Equations and the Bulk Viscosity of Simple Gases," *Journal of Mathematical and Physical Sciences*, Vol. 6, 225-261, 1972.
8. B. Grossman and P. Cinnella, "Flux-Split Algorithms for Flows with Non-equilibrium Chemistry and Vibrational Relaxation," *Journal of Computational Physics*, Vol. 88, No. 1, 131-168, 1990.
9. K. A. Fiscko and D. R. Chapman, "Hypersonic Shock Structure with Burnett Terms in the Viscous Stress and Heat Flux," AIAA Paper No. 88-2733, June, 1988.
10. F. E. Lumpkin III, and D. R. Chapman, "A New Rotational Model For Use in Hypersonic Computational Fluid Mechanics," AIAA Paper No. 89-1737, January, 1989.
11. J. G. Parker, "Rotational and Vibrational Relaxation in Diatomic Gases," *Physics of Fluids*, Vol. 2, 449, 1959.

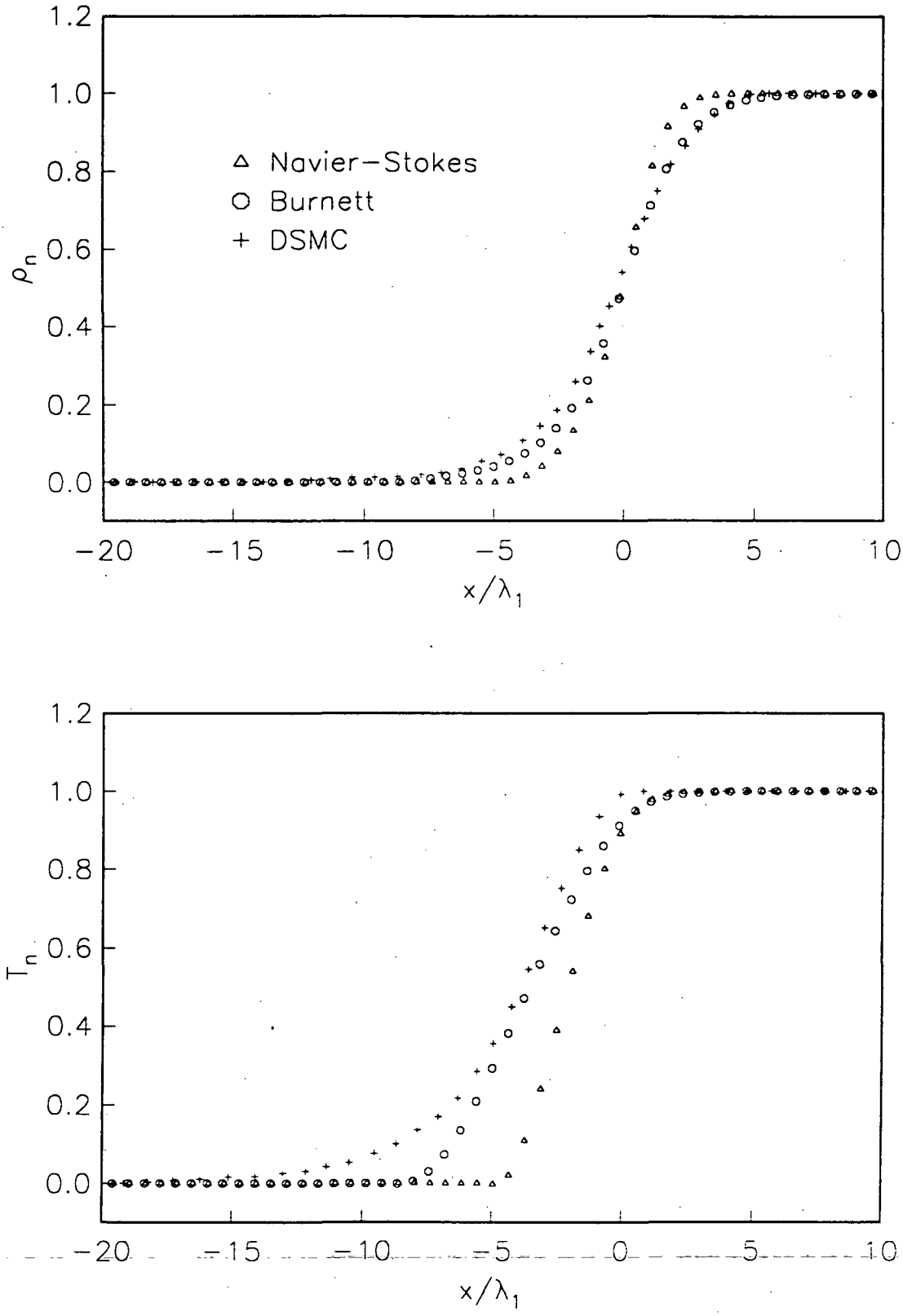


**Figure 1** Density and Temperature Profiles in a Mach 20 Shock for Ar.

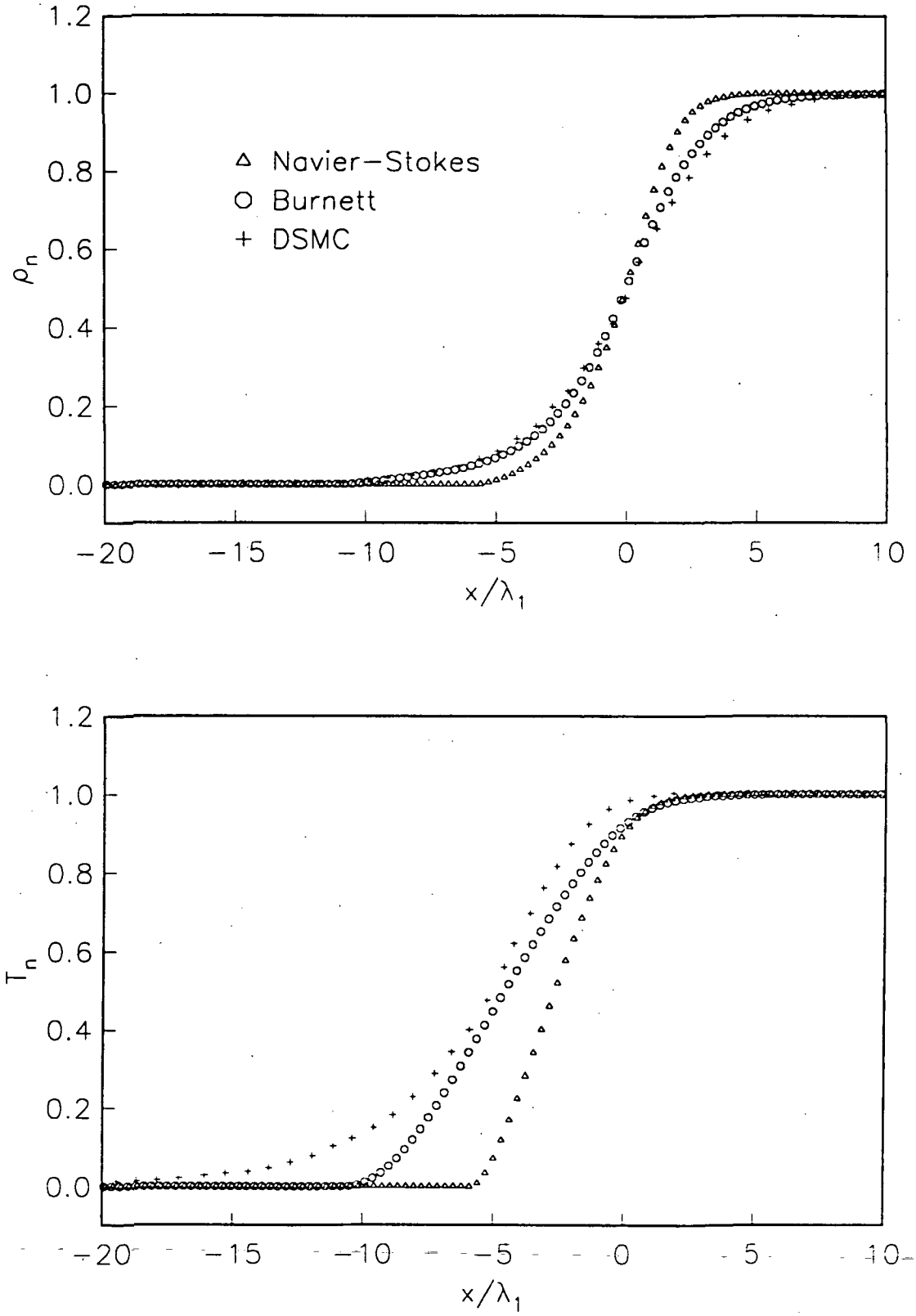


**Figure 2** Density and Temperature Profiles in a Mach 35 Shock for Ar.

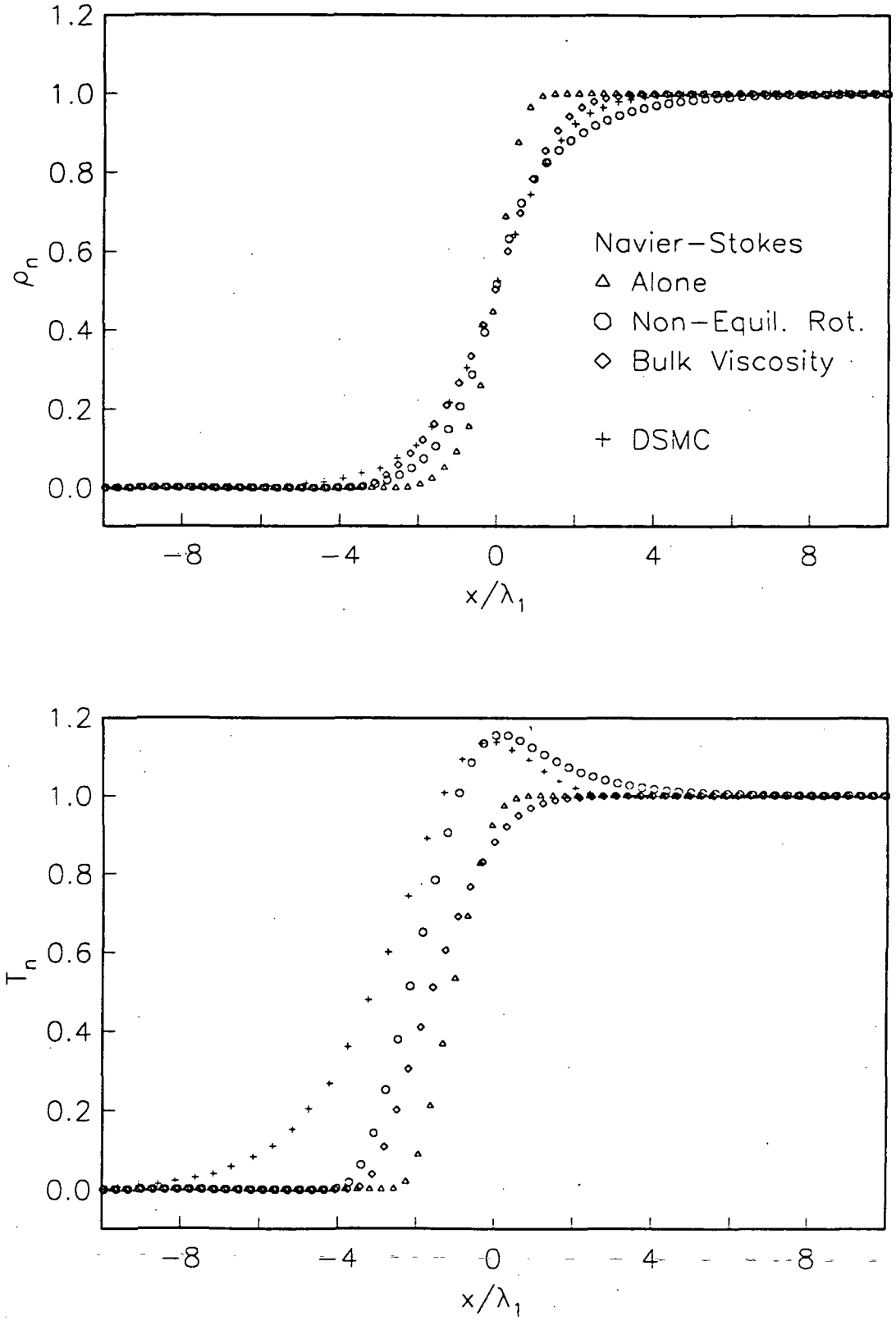


**Figure 3** Density and Temperature Profiles in a Mach 11 Shock for $N_2$.

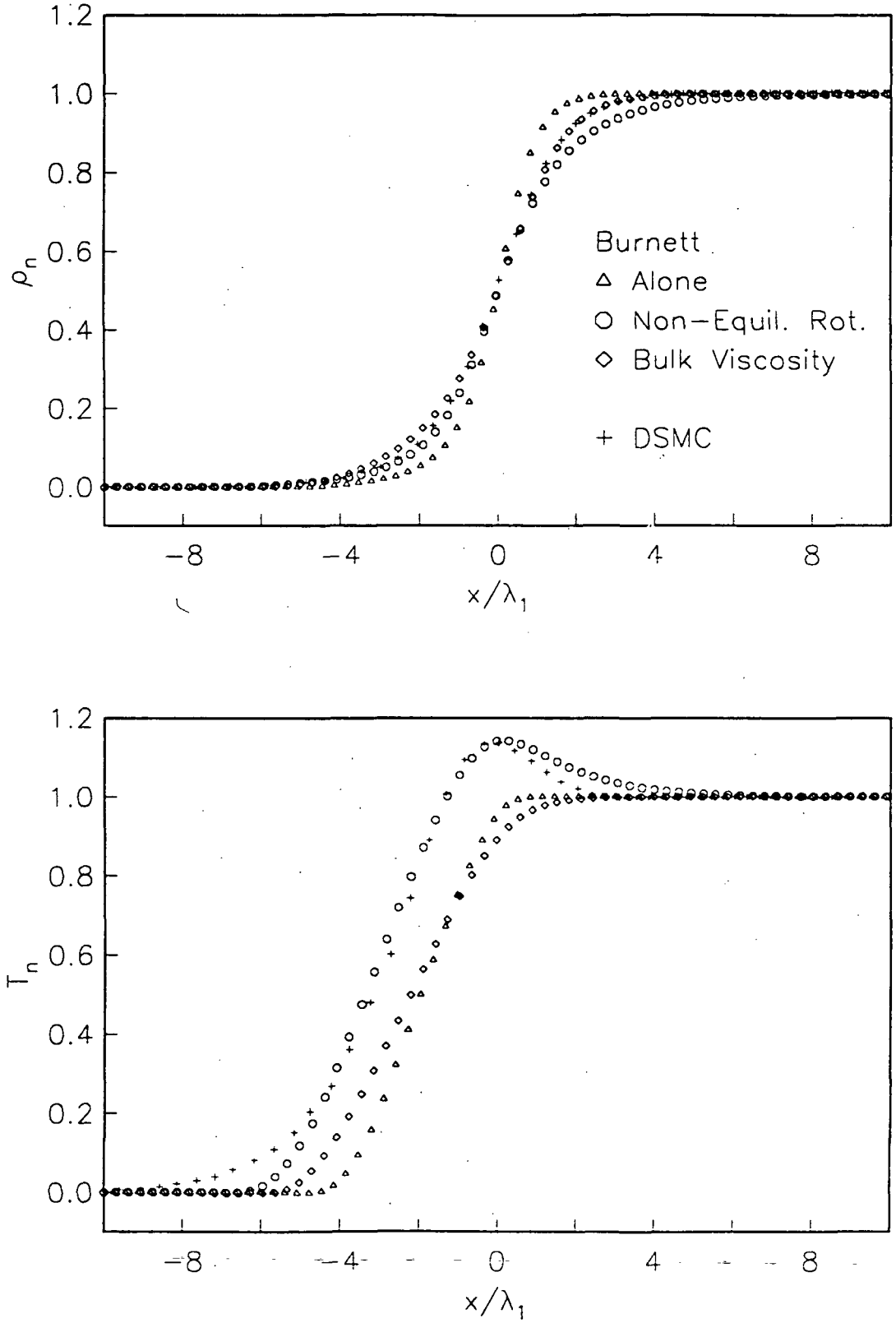


Figure 4 Density and Temperature Profiles in a Mach 11 Shock for $N_2$.

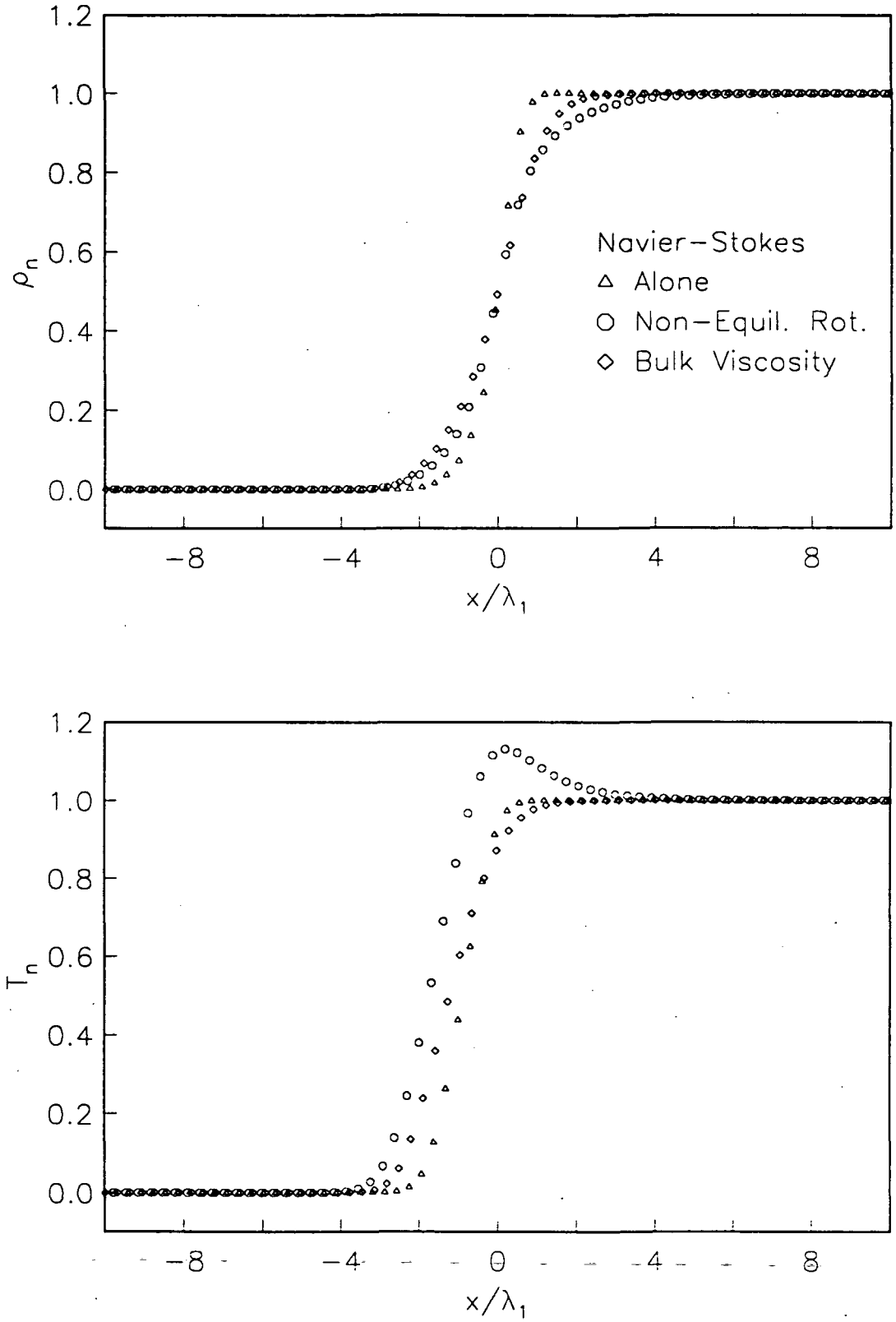


**Figure 5** Density and Temperature Profiles in a Mach 6 Shock for $N_2$.

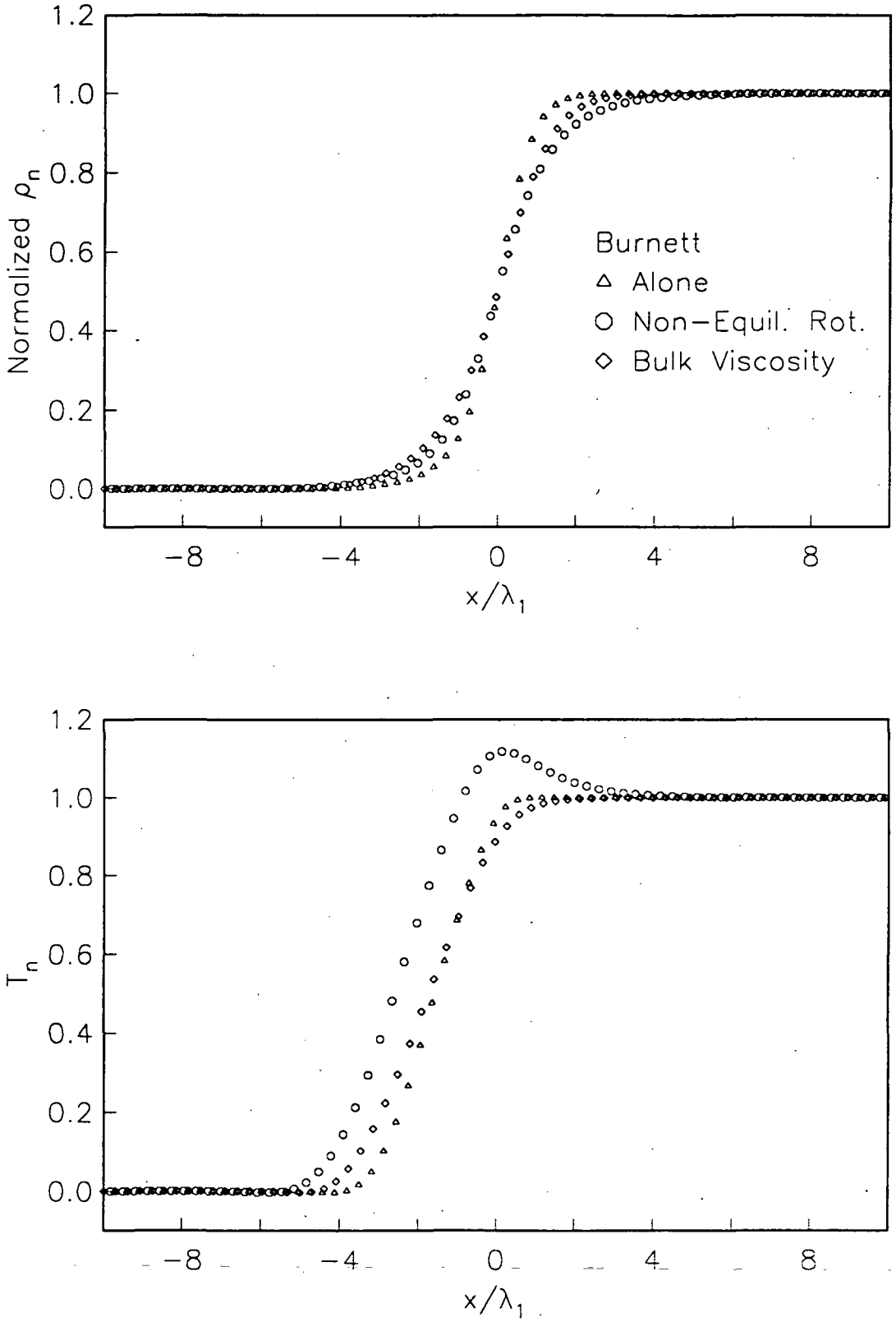


**Figure 6** Density and Temperature Profiles in a Mach 6 Shock for $N_2$.